Beyond the constraints underlying Kolmogorov-Johnson-Mehl-Avrami theory related to the growth laws

M. Tomellini
Dipartimento di Scienze e Tecnologie Chimiche, Università di Roma Tor Vergata, Via della Ricerca Scientifica, I-00133 Roma, Italy

M. Fanfoni
Dipartimento di Fisica, Università di Roma Tor Vergata, Via della Ricerca Scientifica, I-00133 Roma, Italy
(Received 14 October 2011; revised manuscript received 13 December 2011; published 24 February 2012)

The theory of Kolmogorov-Johnson-Mehl-Avrami for phase transition kinetics is subjected to severe limitations concerning the functional form of the growth law. This paper is devoted to sidestepping this drawback through the use of the correlation function approach. Moreover, we put forward an easy-to-handle formula, written in terms of the experimentally accessible actual extended volume fraction, which is found to match several types of growths. Computer simulations have been performed for corroborating the theoretical approach.

DOI: 10.1103/PhysRevE.85.021606 PACS number(s): 68.55.A−, 05.70.Fh, 81.15.Aa

I. INTRODUCTION

The Kolmogorov-Johnson-Mehl-Avrami (KJMA) model [1–3] finds applications in a vast ambit of scientific fields, which range from thin film growth to materials science [4–11] to biology and pharmacology [12,13], let alone the applied probability theory [14,15]. In the majority of these papers, the authors made use of a simplified version of the KJMA formula: the stretched exponential $X(t) = 1 - \exp(-at^n)$, where X is the fraction of the transformed phase and a and n (the latter known as Avrami's exponent) are constants. The model, in principle, is simple because it rests on a Poissonian stochastic process of points in space to which a growth law is attached. In fact, owing to the Poissonian process, the nucleation takes place everywhere in the space, i.e., also in the already transformed phase. This partially fictitious nucleation rate $[I(t)]$, for we are dealing with a Poissonian process, is linked to the actual (real) nucleation rate $[I_a(t)]$ according to $I_a(t) = I(t)[1 - X(t)]$, where $X(t)$ is the transformed fraction. The growth law transforms each point in a nucleus of radius $R(t)$, where t stands for time. The pair, points' generation and growth law, is a key quantity of the theory. It happens that the KJMA model fails for the time-dependent points generation rate (i.e., nucleation rate) associated with diffusional-type growth laws [16,17]. In particular, let us define two classes of growth laws: (i) $d^2R/dt^2 \geqslant 0$ and (ii) $d^2R/dt^2 < 0$. The KJMA model is suitable for describing the first class of growths, and for this reason, we named it KJMA compliant, opposite to the second to which we attach the adjective KJMA noncompliant. The reason for that is due to the particular stochastic process taken into account. As a matter of fact, the Poissonian process requires that points can be generated everywhere throughout the space independently of whether the space is, because of growth, already transformed or not. Points generated in the already transformed space are named phantoms after Avrami. It goes without saying that, in the case of KJMA-compliant growths, phantoms do not contribute to the true transformed fraction, i.e., they are just virtual points whose only role is to simplify the mathematics [18]. On the other hand, in the KJMA-non-compliant growths, phantoms may contribute to the phase transition through the nonphysical overgrowth events [3]. Incidentally, it is worth noticing that the KJMA-non-compliant growths and KJMA-compliant growths are indistinguishable if associated with simultaneous nucleation [19].

According to what has been said, one can summarize saying that the concept of phantom implies the existence of the two classes of growths.

One has to keep in mind that the above stretched exponential expression, $[X(t) = 1 - \exp(-at^n)]$, is the exact solution of the kinetics only in cases $I(t) = constant$ and $I(t) \sim \delta(t)$, where I is the nucleation rate and $\delta(t)$ is Dirac's δ function, provided the growth is according to a power law. In general, the term at^n is a simple way to approximate the convolution product between the nucleation rate (phantom included) and the nucleus volume. This convolution is the extended transformed fraction, $\hat{X}_e$, and takes the contribution of phantoms into account. In view of the extensive use of KJMA theory for dealing with experimental data, it should be desirable to make use of an extended transformed fraction deprived of phantom contribution X_e. A pictorial view of the geometrical meaning of $\hat{X}_e$, X_e, and X is reported in Fig. 1.

The aim of this contribution is twofold: (i) to model the phase transformation kinetics in terms of actual quantities, such as the nucleation rate, (ii) to provide an expression for the transformed fraction as a function of X_e.

II. THEORY

In this section, we discuss the stochastic theory that has to be employed in order to get rid of phantoms in modeling the kinetics of phase transformations ruled by nucleation and growth. To this end, let us define the phantom-included nucleation rate $I(t)$ and the actual nucleation rate $I_a(t)$, namely, the rate of birth of the real nuclei; $I_a(t)$ is the quantity that is experimentally accessible. It goes without saying that a mathematical formulation of the phase transition kinetics, which employs the actual nucleation rate, holds true for both KJMA-compliant and KJMA-non-compliant growth laws. This automatically overcomes the limit of the KJMA approach. However, actual nuclei imply a severe complication of the stochastic nature of the process under study, for we shift from a Poissonian to a non-Poissonian process: In fact,

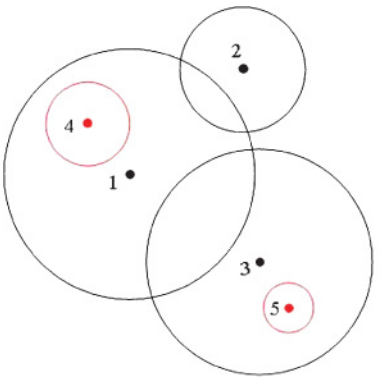

$$X = \left| \cup_{i=1}^{3} X_i \right|$$
$$X_e = X + \left| X_1 \cap (X_3 \cup X_2) \right|$$
$$\hat{X}_e = X_e + |X_4| + |X_5|$$

FIG. 1. (Color online) Pictorial view of a random ensemble of actual (dots 1–3) and phantom (dots 4 and 5) nuclei. The definitions of both phantom-included ($\hat{X}_e$) and actual (X_e) extended fractions also are reported. The (extended) volume of the ith nucleus is denoted as $|X_i|$, and the transformed fraction is denoted as X. The symbol $|A|$ denotes the *cardinality* of the set A.

actual nuclei are correlated spatially. Let us address this point in more detail by denoting the radius of a nucleus with $R(t,t')$ at running time t, which starts growing at time $t' < t$. To be an actual nucleus, it has to lie at a distance $r > R(t',t'')$ from any other older nucleus with $t'' < t'$. In other words, in the spirit of the statistical mechanics of hard spheres, this condition is formalized (at the lowest order) through the pair distribution function for the pair of nuclei (t',t'') at relative distance r,

$$f_2(r,t',t'') \approx H(r - R(t',t'')), \tag{1}$$

where $H(x)$ is the Heaviside function. Throughout the paper, we employ the notation by Van Kampen [20] according to which n-dots distribution and correlation functions are denoted as f_n and g_n, respectively.

In previous papers, we have presented a theory for describing phase transitions in the case of spatially correlated nuclei and for the time-dependent nucleation rate [21,22]. The untransformed fraction can be expressed in terms of either the distribution functions (f_n functions) or the correlation functions (g_n functions) where the f_n's and g_n's are linked by cluster expansion [20]. Given a generic point of space, we have computed the probability that this point is not covered (transformed) by any nucleus up to time t. This probability is the fraction of untransformed phase, i.e., $Q(t) = 1 - X(t)$. By denoting the volume of a nucleus with $|\Delta(t,t')|$, which starts growing at time $t' < t$ at running time t and in the case of symmetric f_n and g_n functions, the uncovered fraction is given by

$$\begin{aligned} Q(t) &= 1 - \int_0^t \tilde{I}(t_1)dt_1 \int_{\Delta(t,t_1)} f_1(\mathbf{r}_1)d\mathbf{r}_1 \\ &\quad + \int_0^t \tilde{I}(t_1)dt_1 \int_0^{t_1} \tilde{I}(t_2)dt_2 \int_{\Delta(t,t_1)} d\mathbf{r}_1 \\ &\quad \times \int_{\Delta(t,t_2)} d\mathbf{r}_2 f_2(\mathbf{r}_1,\mathbf{r}_2) - \cdots \\ &= 1 + \sum_{m=1}^{\infty} \frac{(-1)^m}{m!} \int_0^t \tilde{I}(t_1)dt_1 \cdots \\ &\quad \int_0^t \tilde{I}(t_m)dt_m \int_{\Delta(t,t_1)} d\mathbf{r}_1 \int_{\Delta(t,t_2)} d\mathbf{r}_2 \cdots \\ &\quad \int_{\Delta(t,t_m)} f_m(\mathbf{r}_1,\ldots,\mathbf{r}_m)d\mathbf{r}_m, \end{aligned} \tag{2}$$

or

$$\begin{aligned} Q(t) = \exp\Bigg[&\sum_{m=1}^{\infty} \frac{(-1)^m}{m!} \int_0^t \tilde{I}(t_1)dt_1 \cdots \\ &\int_0^t \tilde{I}(t_m)dt_m \int_{\Delta(t,t_1)} d\mathbf{r}_1 \int_{\Delta(t,t_2)} d\mathbf{r}_2 \cdots \\ &\int_{\Delta(t,t_m)} g_m(\mathbf{r}_1,\ldots,\mathbf{r}_m)d\mathbf{r}_m \Bigg]. \end{aligned} \tag{3}$$

In the case of non symmetric f_n functions, care must be taken on time ordering.

It is worth pointing out that the nucleation rates entering these equations, in fact, are subjected to the condition imposed by the correlation among nuclei. This quantity may or may not imply phantoms depending on the specific form of the f_n functions. For this reason, we introduce the new symbol $\tilde{I}$. In particular, for the hard-core correlation [Eq. (1)], $\tilde{I}$ coincides with the actual nucleation rate $\tilde{I} = I_a$, which leads to the solution of the phase transition kinetics in terms of the actual nucleation rate.

Since [Eqs. (2) and (3)] are the exact solutions of the stochastic process linked to the phase transition, they also coincide with the KJMA formula provided the above mentioned preconditions are met, i.e., random nucleation and KJMA-compliant growth.

As far as the hard-core correlation [Eq. (1)] and the kinetics, Eqs. (2) and (3), are concerned, we note that the number of nuclei of size $R(t,t_1)$ is $I_a(t_1)dt_1 = O(dt_1)$. As a consequence and in the framework of the statistical mechanics of hard sphere fluid, we are dealing with an extremely dilute solution of pairs of components t_1,t_2. Accordingly, because the number density of t_2 spheres is on the order of $O(dt_2)$, higher order terms in the cluster expansion of the f_2 function can be neglected, thus, $f_2(r,t',t'') = H(r - R(t',t''))$ in Eq. (2).

A. KJMA-compliant growths

In this section, we show that Eq. (2) is compatible with the KJMA kinetics only in the case of a KJMA-compliant function. On the other hand, such a comparison will give deeper insight into the reasons why the KJMA kinetics does not work in the case of KJMA-non-compliant functions. In the following, we discuss the linear growth law for the two-dimensional (2D) case. Also, to simplify the complexity of the computation, the actual nucleation rate I_a is taken as a constant; as a consequence, the phantom-included nucleation rate reads [3,19] $I(t) = I_a/[1 - X(t)] = I_a/Q(t) \equiv I_a F(t)$, and the KJMA kinetics becomes

$$F(t) = \exp\left[\int_0^t I_a F(t')\pi R^2(t,t')dt' \right], \tag{4}$$

where $R(t,t') = v(t - t')$ and v is a constant.

We consider the series expansion of $F(t)$ around $t = 0$. One gets

$$\frac{d^{n+1}F(t)}{dt^{n+1}} \equiv F^{(n+1)} = (F\Omega)^{(n)} = \sum_{k=0}^{n} \binom{n}{k} F^{(n)}\Omega^{(n-k)}, \quad (5)$$

where $\Omega(t) = 2\pi I_a \int_0^t F(t')R(t,t')\partial_t R(t,t')dt' = 2\pi I_a v \int_0^t F(t')R(t,t')dt'$.

Moreover, since $\Omega^{(m+2)} = \kappa F^{(m)}$, where $\kappa = 2\pi v^2 I_a$ and $F^{(0)} = 1$ and $\Omega^{(0)} = \Omega^{(1)} = 0$, from Eq. (5), it is found that only the terms $F^{(3n)}(0)$ are different from zero, i.e., $F(t) = \sum_{n=0}^{\infty} \frac{1}{(3n)!} F^{(3n)}(0)\, t^{3n} = \sum_{m=0}^{\infty} c_m t^m$. In particular, the first coefficients are as follows: $F^{(3)}(0) = \kappa$, $F^{(6)}(0) = 11\kappa^2$, $F^{(9)}(0) = 375\kappa^3$, and $F^{(12)}(0) = 234\,147\kappa^4$.

Next, we derive the series expansion of the untransformed fraction $Q(t) = \sum_{n=0}^{\infty} b_n t^n$ by exploiting the condition $1 = Q(t)F(t) = \sum_{n=0}^{\infty} b_n t^n \sum_{m=0}^{\infty} c_m t^m$. Even in this case, the b_n coefficients are different from zero for $n = 3k$ (with integer k). The first four coefficients are

$$\begin{aligned} &b_0 = \frac{1}{c_0} = 1, \quad b_3 = -c_3, \\ &b_6 = -c_6 + c_3^2, \quad b_9 = -c_9 + 2c_3c_6 - c_3^2. \end{aligned} \quad (6)$$

By using the expression of c_n's, the series of the untransformed fraction up to t^9 is given as

$$Q(t) = 1 - \frac{1}{6}\kappa t^3 + \frac{1}{80}\kappa^2 t^6 - \frac{207}{9!}\kappa^3 t^9 + O(t^{12}). \quad (7)$$

Since $X_e = \frac{1}{3!}\kappa t^3 = \frac{1}{3}\pi I_a v^2 t^3 = \int_0^t I_a \pi R^2(t,t')dt'$, the series, Eq. (7), can be rewritten as

$$Q(t) = 1 - X_e + \tfrac{9}{20}X_e^2 - \tfrac{69}{560}X_e^3 + O\left(X_e^4\right), \quad (8)$$

where the last two coefficients are 0.45 and 0.123. We emphasize that the coefficients of this series only depend upon the growth law for the constant I_a (see also the last section).

The next step is to show that the untransformed fraction, given by the series, Eq. (2), is equal to Eq. (7) or Eq. (8). We have carried out the first two terms, exactly, while, owing to the tremendous computational complexity for the third term, an approximation has been employed. It is worth being reminded that the distribution functions are $f_1(\mathbf{r}_1) = 1$, $f_2(\mathbf{r}_{12},t_1,t_2) = H(r_{12} - R(t_1,t_2))$, and $f_3(\mathbf{r}_{12},\mathbf{r}_{13},\mathbf{r}_{23},t_1,t_2,t_3) = H(r_{12} - R(t_1,t_2))H(r_{13} - R(t_1,t_3))H(r_{23} - R(t_2,t_3))$, where $\mathbf{r}_{ij}$ is the relative distance. In fact, since $I_a dt_i = O(dt_i)$, the system of dots is dilute, and $f_3(1,2,3) = f_2(1,2)f_2(1,3)f_2(3,2)$, i.e., the superposition principle holds true [23]. Since the system is homogeneous, the f_n functions depend on $r_{ij} = |\mathbf{r}_{ij}| = |\mathbf{r}_i - \mathbf{r}_j|$. Equation (2) becomes

$$\begin{aligned} Q(t) = 1 &- I_a \int_0^t dt_1 \int_{\Delta(t,t_1)} d\mathbf{r}_1 + I_a^2 \int_0^t dt_1 \int_0^{t_1} dt_2 \\ &\times \int_{\Delta(t,t_1)} d\mathbf{r}_1 \int_{\Delta(t,t_2)} d\mathbf{r}_2 H(r_{12} - R(t_1,t_2)) \\ &- I_a^3 \int_0^t dt_1 \int_0^{t_1} dt_2 \int_0^{t_2} dt_3 \int_{\Delta(t,t_1)} d\mathbf{r}_1 \int_{\Delta(t,t_2)} d\mathbf{r}_2 \end{aligned}$$

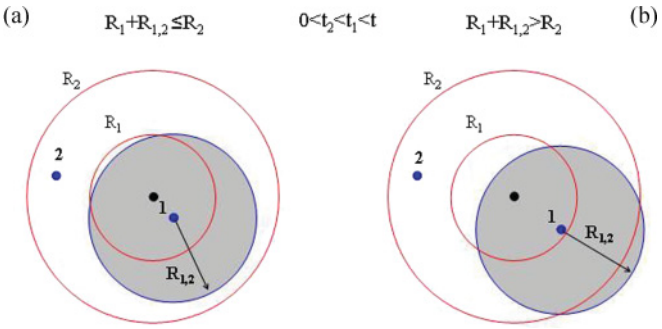

FIG. 2. (Color online) The integration domains and the correlation circles are depicted for the integrals over the f_2 function. The cases of KJMA-compliant and KJMA-non-compliant growths are reported in panels (a) and (b), respectively. In the drawing, $R_{1,2} \equiv R(t_1,t_2)$, $R_i \equiv R(t,t_i)$ $(i = 1,2)$, and $t_2 < t_1$. In the case of KJMA-compliant growths, (a) $R_1 + R_{1,2} \leqslant R_2$, and the hard-core circle is within the integration domain R_2. In the case of KJMA-non-compliant growths, (b) $R_1 + R_{1,2} > R_2$, and the hard-core disk overcomes the integration domain of the older nucleus.

$$\begin{aligned} &\times \int_{\Delta(t,t_3)} d\mathbf{r}_3 H(r_{12} - R(t_1,t_2))H(r_{23} - R(t_2,t_3)) \\ &\times H(r_{13} - R(t_1,t_3)) + \cdots, \end{aligned} \quad (9)$$

where the integration domain $\Delta(t,t_i)$ is the circle of radius $R(t,t_i) = v(t - t_i)$. The f_1 containing term is the extended surface fraction $X_e(t) = I_a \int_0^t dt_1 |\Delta(t,t_1)|$ and coincides with the second term of the expansion, Eq. (8). Let us focus our attention on the integrals in the spatial domain—for the sake of clarity shown in Fig. 2(a) together with the circle of correlation $R(t_1,t_2)$—of the f_2 containing term. By employing relative coordinates, the integrals read

$$\begin{aligned} &\int_{\Delta(t,t_1)} d\mathbf{r}_1 \int_{\Delta(t,t_2)} d\mathbf{r}_{12} H(r_{12} - R(t_1,t_2)) \\ &\quad = \int_{\Delta(t,t_1)} d\mathbf{r}_1 A(r_1,t,t_1,t_2), \end{aligned} \quad (10)$$

where $A(r_1,t,t_1,t_2) = A(r_1,R(t,t_2),R(t_1,t_2))$ is the area spanned by the second nucleus when the first one is located at $\mathbf{r}_1$ $(t_2 < t_1 < t)$. It is at this point of the computation that the growth law comes into play; indeed, in the case of KJMA-compliant growth laws (here linear growth), the correlation circle $R(t_1,t_2)$ is entirely within the integration domain $R(t,t_2)$ [Fig. 2(a)]. Consequently,

$$A(t,t_1,t_2) = \pi[R^2(t,t_2) - R^2(t_1,t_2)] \quad (11)$$

is independent of $\mathbf{r}_1$. On the other hand, in the case of KJMA-non-compliant growth laws, the correlation circle overcomes the integration domain of the second nucleus, and the relationship above does not hold true anymore [see Fig. 2(b)]. In general, the KJMA-compliant functions satisfy the condition $R(t,t_1) + R(t_1,t_2) \leqslant R(t,t_2)$, i.e., for a power growth law $(t - t_1)^n + (t_1 - t_2)^n \leqslant (t - t_2)^n$, which is verified only for $n \geqslant 1$. In fact, by setting $\tau = t_1 - t_2$ and $\eta = \frac{t - t_2}{\tau} > 1$, the inequality above reads $(\eta - 1)^n \leqslant \eta^n - 1$, which is satisfied for $n \geqslant 1$. On the other hand, for $n = 1/k$ (with integer $k > 1$), the inequality is $[(\eta - 1)^{1/k} + 1]^k \leqslant \eta$,

namely,

$$\sum_{\mu=1}^{k-1}\binom{k}{\mu}(\eta-1)^{\mu/k}\leqslant 0, \tag{12}$$

which is never satisfied ($\eta>1$).

For the KJMA-compliant growth, the contribution of the f_2 containing term becomes

$$\begin{aligned}\pi I_a^2\int_0^t dt_1\int_0^{t_1}dt_2\int_{\Delta(t,t_1)}d\mathbf{r}_1[R^2(t,t_2)-R^2(t_1,t_2)] &= \pi^2 I_a^2\int_0^t dt_1\int_0^{t_1}dt_2 R^2(t,t_1)[R^2(t,t_2)-R^2(t_1,t_2)]\\ &= \frac{X_e^2}{2}-\pi^2 I_a^2\int_0^t dt_1\int_0^{t_1}dt_2 R^2(t,t_1)R^2(t_1,t_2).\end{aligned} \tag{13}$$

It is possible to show that, for linear growth, the last term of Eq. (13) is equal to $\frac{1}{180}(\pi I_a v^2 t^3)^2$; consequently, we get $\frac{X_e^2}{2}-\frac{9X_e^2}{180}=\frac{9}{20}X_e^2$, which coincides with the term of the same order in the KJMA series, Eq. (8).

Let us now briefly consider the contribution of the f_3 containing term in the general expression, Eq. (2). Figure 3 shows the integration domains $R_i=R(t,t_i)$ and the correlation circles $R(t_i,t_j)$ for the three nuclei born at time t_i ($i=1,2,3$). The configuration integral over f_3 in Eq. (9) becomes

$$\begin{aligned}&I_a^3\int_0^t dt_1\int_0^{t_1}dt_2\int_0^{t_2}dt_3\int_{\Delta(t,t_1)}d\mathbf{r}_1\int_{\Delta(t,t_2)}d\mathbf{r}_2 H(r_{12}-R(t_1,t_2))\int_{\Delta(t,t_3)}d\mathbf{r}_3 H(r_{13}-R(t_1,t_3))H(r_{23}-R(t_2,t_3))\\ &= I_a^3\int_0^t dt_1\int_0^{t_1}dt_2\int_0^{t_2}dt_3\int_{\Delta(t,t_1)}d\mathbf{r}_1\int_{\Delta(t,t_2)}d\mathbf{r}_2 H(r_{12}-R(t_1,t_2))A(r_{12},R(t_1,t_3),R(t_2,t_3)),\end{aligned} \tag{14}$$

where $t_3<t_2<t_1<t$ is assumed. In this equation, $A(r_{12},R(t_1,t_3),R(t_2,t_3))$ is the area spanned by the third nucleus when the first and second ones are located at $\mathbf{r}_1$ and $\mathbf{r}_2$, respectively. Because of the possible overlap between the correlation circles $R(t_1,t_3)$ and $R(t_2,t_3)$ and for $R(t_1,t_3)$ encompassed within $R(t,t_3)$, this area is a function of r_{12} as

$$\begin{aligned}A(r_{12}) &= \omega(r_{12})H[R(t_1,t_3)+R(t_2,t_3)-r_{12}]\\ &\quad+\pi[R^2(t,t_3)-R^2(t_1,t_3)-R^2(t_2,t_3)]\\ &\quad\times H(r_{12}-R(t_2,t_3)-R(t_1,t_3)),\end{aligned} \tag{15}$$

where $\omega(r_{12})=\pi[R^2(t,t_3)-R^2(t_1,t_3)-R^2(t_2,t_3)]+\varpi(r_{12},R(t_1,t_3),R(t_2,t_3))$ with $\varpi(x,\rho_1,\rho_2)$ being the overlap area of two circles of radii ρ_1 and ρ_2 at relative distance x,

$$\begin{aligned}\varpi(x,\rho_1,\rho_2) &= -\frac{1}{2}\sqrt{4x^2\rho_1^2-\left[\rho_2^2-x^2-\rho_1^2\right]^2}\\ &\quad+\rho_1^2\arccos\frac{\rho_1^2+x^2-\rho_2^2}{2x\rho_1}\\ &\quad+\rho_2^2\arccos\frac{\rho_2^2+x^2-\rho_1^2}{2x\rho_2}.\end{aligned} \tag{16}$$

It turns out that the computation of the third order term of the series, Eq. (14), is a formidable task indeed. We do not attempt to perform the exact estimate of this term, which, however, must coincide with the same order term of the KJMA series. On the other hand, an approximate evaluation of this term, by using an oversimplified form of the $A(r_{12})$ area, is possible by formally rewriting this area as $A(r_{12})=\pi[R^2(t,t_3)-R^2(t_1,t_3)-\beta R^2(t_2,t_3)]$, where $\beta\in(0,1)$ is given by $\beta=\{1-\frac{\varpi(r_{12})}{\pi R^2(t_2,t_3)}H[R(t_1,t_3)+R(t_2,t_3)-r_{12}]\}$. In the case of complete overlap ($\beta=0$), we get

$$\begin{aligned}&\pi^3 I_a^3\int_0^t dt_1\int_0^{t_1}dt_2\int_0^{t_2}dt_3 R^2(t,t_1)[R^2(t,t_2)\\ &\quad-R^2(t_1,t_2)][R^2(t,t_3)-R^2(t_1,t_3)],\end{aligned} \tag{17}$$

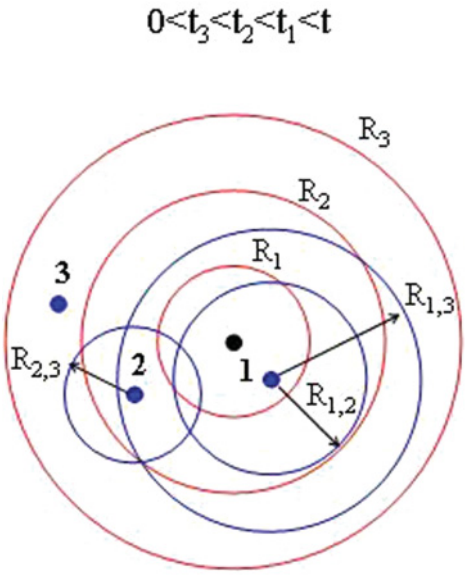

FIG. 3. (Color online) Integration domains and correlation hard disks for the integral over the f_3 function. In the drawing, $R_{i,j}\equiv R(t_i,t_j)$ and $R_i\equiv R(t,t_i)$. In the case of KJMA-compliant growth, all the circles are entirely within the $R(t,t_3)$ circle.

which, for the linear growth $[R(t,t') = v(t-t')]$, gives $\frac{24}{7!} I_a^3 \pi^3 v^6 t^9 = \frac{72}{560} X_e^3$ to be compared with the exact value $\frac{69}{560} X_e^3$, which brings an uncertainty of 4.3%.

B. KJMA-non-compliant growths

Let us now consider the parabolic growth $R(t,t') = v\sqrt{t-t'}$. In this case, the series expansion of the function $F(t) = 1/Q(t)$, given by Eq. (4), can be performed by employing the same computation pathway discussed above where now $\Omega^{(n+1)} = \kappa F^{(n)}$ and $\kappa = \pi I_a v^2$. In this case, $F^{(2n)}(0) \neq 0$ implies $F(t) = 1 + \frac{\kappa}{2}t^2 + \frac{1}{6}\kappa^2 t^4 + \frac{34}{6!}\kappa^3 t^6$ and

$$Q(t) = 1 - \frac{\kappa}{2}t^2 + \frac{\kappa^2}{12}t^4 - \frac{\kappa^3}{180}t^6 + O(t^8) = 1 - X_e + \frac{1}{3}X_e^2 - \frac{4}{90}X_e^3 + O\left(X_e^4\right), \quad (18)$$

where the two last coefficients are 0.33 and 0.044. It is worth pointing out that, in such an evaluation, the transformed fraction X is comprehensive of the contribution of phantoms. In fact, we recall that Eq. (4) is the KJMA solution with the phantom-included nucleation rate $I_a/(1-X)$.

The f_1 containing term of Eq. (2) gives the extended volume fraction $\frac{\kappa}{2}t^2$. As far as the third term is concerned (f_2 contribution), it also is possible to show that, for $n = 1/2$, the integral, Eq. (13), coincides with the third term of Eq. (18), $\frac{\kappa^2}{12}t^4$. However, it is important to stress that, in this case, Eq. (13) does not coincide with the integral over the f_2 function of the exact solution, Eq. (9) since, in the latter equation, we only enter the actual nuclei. From the mathematical point of view, in the case of parabolic growth, the correlation circle is not contained within the integration domain as depicted in Fig. 2(b). In other words, for KJMA-non-compliant growth laws, area A is a function of r_1, and the term of order I_a^2 in Eq. (9) does not coincide with $\frac{X_e^2}{3}$ of Eq. (18) (parabolic growth). In particular, under these circumstances, we get

$$A(r_1,t,t_1,t_2) = \omega(r_1)H(r_1 + R(t_1,t_2) - R(t,t_2)) + \pi[R^2(t,t_2) - R^2(t_1,t_2)]H[R(t,t_2) - r_1 - R(t_1,t_2)], \quad (19)$$

where $\omega(r_1) = \pi R^2(t,t_2) - \varpi(r_1, R(t,t_2), R(t_1,t_2))$ with $\varpi(r_1)$ as the overlap area of two circles of radii $R(t,t_2)$ and $R(t_1,t_2)$ at distance r_1 [Eq. (16)].

III. NUMERICAL SIMULATIONS

The ultimate aim of this section is to propose a simple formula for describing the kinetics on the basis of the actual extended transformed fraction X_e. On the grounds of Eq. (3), the transformed fraction can be rewritten in the general form

$$X(t) = 1 - \exp\{-X_e(t)\gamma[X_e(t)]\}, \quad (20)$$

where $\gamma[X_e(t)]$ embodies the contributions of correlations among nuclei [21]. It is worth noticing that, for KJMA-complaint growths (random nucleation), Eq. (3) actually reproduces the KJMA formula. In fact, by identifying $\tilde{I}$ with the phantom-included nucleation rate ($\tilde{I} \equiv I$), one gets $g_{m>1} = 0$ leading to the formula $Q = \exp(-\hat{X}_e)$. On the other hand, working with the actual nucleation rate, in Eq. (3), $\tilde{I} \equiv I_a$ and $g_m \neq 0$, and the series has infinite terms. Therefore, $\gamma[X_e(t)]$ can be expanded as a power series of the extended actual volume fraction X_e. Moreover, by exploiting the homogeneity properties of the f_n functions (see below), it is possible to attach a physical meaning to the power series coefficients in terms of nucleation rate and growth law. Also, for constant I_a, the coefficients of this series only depend upon growth law. For the aim of achieving a suitable compromise between handiness and pliability, we retain the linear approximation of $\gamma[X_e(t)]$ by obtaining the following kinetics:

$$X = 1 - \exp\left[-\left(aX_e + bX_e^2\right)\right], \quad (21)$$

with a and b as constants. For the sake of completeness, we point out that, according to its physical meaning, parameter a should be unitary. Nevertheless, the substitution of the infinite expansion with only two terms authorizes the introduction of the new parameter a. In any case, the a values are found to be nearly 1 [see Fig. 7 below].

In order to study the transition kinetics in terms of actual nuclei and to test Eq. (21), we worked out 2D computer simulations for several growth laws at the constant nucleation rate I_a.

Typically, for these kinds of papers [5,24], the simulation is performed on a lattice (square in our case) where, in order to mimic the continuum case, the lattice space is much lower than the mean size of the nuclei.

In particular, the transformation takes place on a square lattice whose dimension is 1000×1000 with a nucleation rate of $I_a = 3$. It is worth being reminded that, since the nucleation is Poissonian, it occurs on the entire lattice independent of whether the space is transformed already or not. The computer simulation can be run either taking the presence of phantoms into account or not. In the former case, the outputs have been labeled as with "w," whereas, the latter have been labeled as without "wo." As far as the growth laws are concerned, we limited ourselves to the power laws $R(t) \sim t^n$ for $n = 1/4,\ 1/3,\ 1/2,\ 1,\ 3/2$, and 2.

The results of the simulations for the KJMA-non-compliant growths are displayed in Figs. 4(a)–4(c). In particular, the fractional surface coverage X, as a function of the actual extended fraction X_e, with and without the contribution of phantoms, are reported (curves labeled with w and wo, respectively). The contribution of phantom overgrowth to the transformation kinetics is highlighted in Fig. 5 and shows that this effect brings an uncertainty to X, which ranges from 2 to 5% ongoing from $n = 1/2$ to $n = 1/4$. In the case of parabolic growth, this figure is lower than 2%. These results are in qualitative agreement with previous papers on phantom overgrowth, although performed for different nucleation laws [16,24]. As discussed in more detail below, the results displayed in Figs. 4 and 5 are universal, i.e., they only depend on power exponent n and the nucleation law (in the present case, $I_a = constant$). Accordingly, the lower n, the more important phantom overgrowth. In fact, let us consider a phantom, which starts growing at time $\bar{t}$, located at r_p from the center of an actual nucleus, which starts growing at $t = 0$ [Fig. 6(a)]. For KJMA-non-compliant growth $R(t-t') = v(t-t')^{1/k}$ (with integer $k > 1$), the phantom

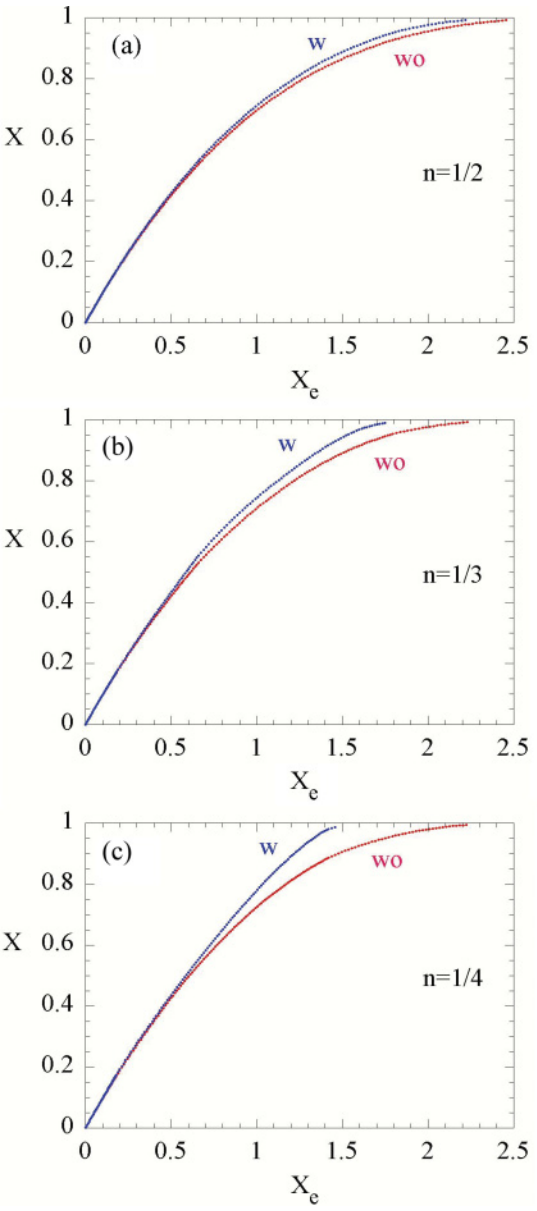

FIG. 4. (Color online) Computer simulations of phase transformations ruled by KJMA-non-compliant growths. The surface fraction X is shown as a function of the extended fraction X_e for the power law ($R \approx t^n$) where $n = 1/2$, $1/3$, and $1/4$ in (a)–(c), respectively. The kinetics with (w) and without (wo) the inclusion of phantoms are displayed.

overtakes the actual nucleus at time t_o, that is, the solution of equation $r_p + v(t_o - \bar{t})^{1/k} = vt_o^{1/k}$, namely,

$$\xi = \eta^{1/k} - (\eta - 1)^{1/k}, \tag{22}$$

where $\xi = \frac{r_p}{v\bar{t}^{\frac{1}{k}}} < 1$ and $\eta = \frac{t_o}{\bar{t}} > 1$. The graphical solution of Eq. (22) is depicted in Fig. 6(b) and indicates that t_o (and, therefore, η) decreases with k. This is in agreement with the results of Fig. 5, which show that the overgrowth phenomenon is more important at greater k.

As far as the guess function, Eq. (21), is concerned, it matches the simulation curves with a very high degree of correlation. For instance, the output of the fit to the $n = 2$ curve gives $a = 0.9750 \pm 0.0007$, $b = 0.088 \pm 0.001$, and a squared correlation coefficient practically 1. For the sake of completeness, the a and b fitting parameters are shown in Fig. 7 where a is found to be nearly 1. This is in agreement with the theoretical value predicted by Eq. (3).

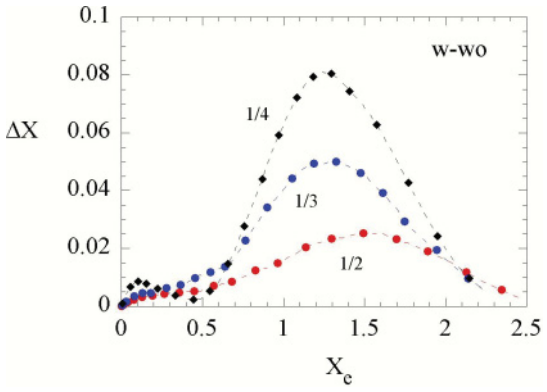

FIG. 5. (Color online) Contribution of phantom overgrowth to the kinetics reported in Fig. 4 [displayed is the difference between curves (w) and (wo)]. The area beneath the curves, normalized to the area of the kinetics of Fig. 4, are 0.053, 0.038, and 0.02 for $n = 1/4$, $n = 1/3$, and $n = 1/2$, respectively.

The behavior of the transformed fraction for KJMA-compliant growths is reported in Fig. 8 for $n = 1$, $n = 3/2$, and $n = 2$. These kinetics are very close to each other and differ markedly from that at $n = 1/2$ also reported in the same figure. In the inset, the kinetics for $n = 1/2$ and $n = 1$ are compared with the KJMA series expansions, Eqs. (18) and (8), respectively. The fact that the curves for $n = 1$, $3/2$, and 2 collapse on the same curve can be rationalized by computing the coefficients of the series expansion of $Q(X_e)$ for integer n. In particular, by employing the method discussed in the previous section, the last two coefficients of the series

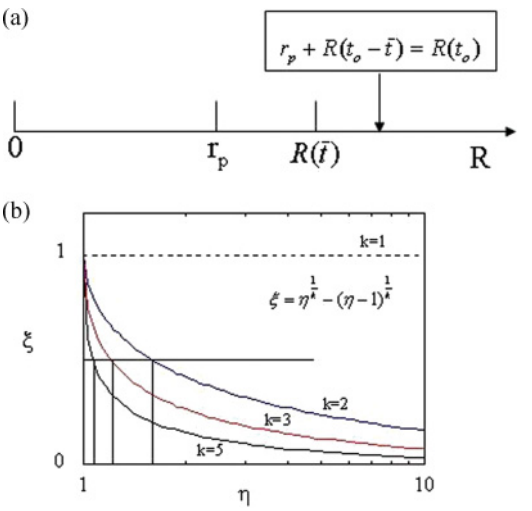

FIG. 6. (a) Sketch of the overgrowth process in the space domain. r_p denotes the location of the phantom, which starts growing at time $\bar{t}$ when the size of the actual nucleus is $R(\bar{t})$. The phantom overtakes the actual nucleus at time t_o when the size of the actual nucleus is $R(t_o)$. (b) Graphical solution of Eq. (22) for the determination of $\eta = \frac{t_o}{\bar{t}} > 1$.

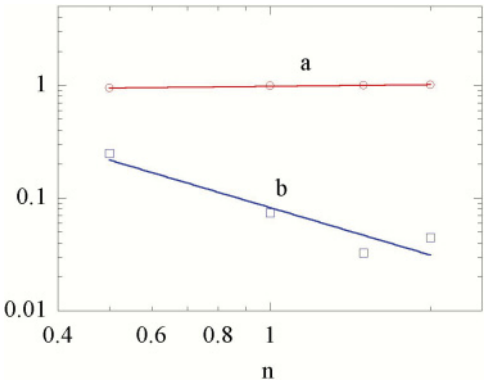

FIG. 7. (Color online) Behavior of the fitting parameters a and b of Eq. (21) as a function of growth exponent n for KJMA-non-compliant growths.

[e.g., Eq. (8)] are 0.4960, 0.1633 and 0.5, 0.1673 for $n = 2$ and 3, respectively. We also performed computer simulations of phase transitions for the nonconstant actual nucleation rate. The output of this computation is displayed in Fig. 9 where the behavior of the nucleation rate is also shown as a function of X_e. In particular, the actual nucleation rate is given by the function $I_a(t) \approx t^2 \exp(-\tilde{a}t^3)$. Also, in this case, the function, Eq. (21), has been found to match the kinetics with a high degree of correlation where, again, the independent variable is the actual extended surface fraction.

Let us address, in more detail, the question of the dependence of volume fraction on extended volume fraction. To this end, we discuss the second order term of the exact solution of Eq. (2), namely,

$$\int_0^t I_a(t')dt' \int_0^{t'} I_a(t'')dt'' \int_{\Delta(t,t')} d\mathbf{r}_1 A(r_1, R(t',t''), R(t,t'')), \tag{23}$$

where Eq. (10) has been employed. We point out that, in Eq. (23), $A(r_1, R(t',t''), R(t,t''))$ is a second order homogeneous function of r_1, $R(t',t'')$, and $R(t,t'')$ variables.

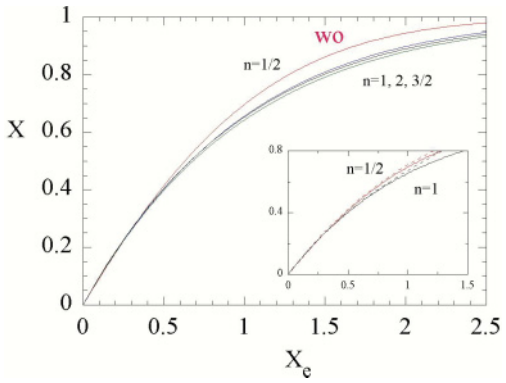

FIG. 8. (Color online) Kinetics of the actual surface fraction as a function of the actual extended surface fraction for several values of n. In the graph, the kinetics for $n = 1/2$ is compared with the KJMA-compliant growth with $n = 1$, $n = 2$, and $n = 3/2$ (from the top, respectively). In the inset, the kinetics for $n = 1$ and $n = 1/2$ are displayed together with the truncated KJMA series expansions, Eqs. (8) and (18), respectively.

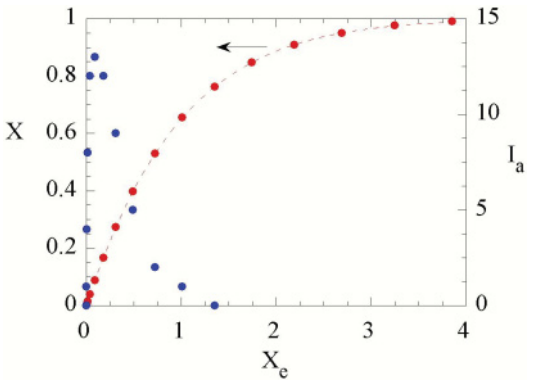

FIG. 9. (Color online) Kinetics of the actual surface fraction as a function of the actual extended surface for the nonconstant actual nucleation rate (left scale). The best fit of the function, Eq. (21), to the $X(X_e)$ kinetics has been shown as a dashed line. The correlation coefficient of the fit is, in fact, 1 for the parameters $a = 1.014$ and $b = 0.0382$. The actual nucleation rate as a function of X_e also is reported on the right scale in $nuclei \times 10^6/site$ units.

Accordingly, for the growth law $R(t,t') = v(t-t')^n$, using the rescaled variables $r_1' = r_1/vt^n$, $\tau' = t'/t$, and $\tau'' = t''/t$, the integral becomes

$$\pi^2 v^4 t^{4n+2} \int_0^1 I_a(\tau')d\tau' \int_0^{\tau'} I_a(\tau'')d\tau'' \int_{\Delta(\tau')} d\mathbf{r}_1' A(r_1', \tau', \tau''). \tag{24}$$

Equation (24) takes the form $C_2 X_e^2$ where

$$C_2\{n,[I_a(\tau)]\} = \frac{\int_0^1 d\tau' I_a(\tau') \int_0^{\tau'} I_a(\tau'')d\tau'' \int_{\Delta(\tau')} A(r_1', \tau', \tau'')d\mathbf{r}_1'}{\left[\int_0^1 I_a(\tau')(1-\tau')^{2n}d\tau'\right]^2}$$

depends on n and the actual nucleation rate. It is apparent that, in the case discussed in the previous section, $I_a(t) = I_a, C_2(n)$ as well as higher order coefficients are a function of n only. In this case, the transformed fraction is expected to be of the form $1 - X = \sum_k C_k(n) X_e^k$.

On the other hand, in the case of a constant phantom-included nucleation rate, $I_a(t) = I_0[1 - X(t)] = I_0 Q(t)$, and Eq. (2) becomes an integral equation for the $Q(t)$ unknown. With reference to the second order term, in this case, Eq. (24) takes the general form $C'(n)\hat{X}_e^2$, which now implies the series $1 - X = \sum_k C_k'(n)\hat{X}_e^k$ (note that this is a series expansion in terms of the phantom-included extended surface). In the specific case of KJMA-compliant growths, however, these series reduce to the exponential series with constant coefficients $\frac{(-1)^k}{k!}$. It is instructive to estimate the first two coefficients in the case of linear growth. For the constant phantom-included nucleation rate, the untransformed fraction satisfies the integral equation,

$$Q(t) = 1 - I_0 \int_0^t Q(t')|\Delta(t,t')|dt' + I_0^2 \int_0^t dt' \int_0^{t'} dt'' Q(t')Q(t'') \times \int_{\Delta(t,t')} d\mathbf{r}_1 A(r_1, t, t', t'') + O\left(I_0^3\right). \tag{25}$$

The first order term of this equation, namely, on the order of I_0, gives $Q(t) = 1 - I_0 \pi v^2 t^3/3 = 1 - \hat{X}_e$. By substituting $Q \approx 1 - \hat{X}_e$ in Eq. (25), we get

$$Q(t) = 1 - \hat{X}_e + I_0 \int_0^t \hat{X}_e(t')|\Delta(t,t')|dt' + I_0^2 \int_0^t dt' \int_0^{t'} dt'' \times \int_{\Delta(t,t')} d\mathbf{r}_1 A(r_1,t,t',t'') + O\left(I_0^3\right). \quad (26)$$

Using dimensionless variables $r_1' = r_1/vt$, $\tau' = t'/t$, and $\tau'' = t''/t$, Eq. (26) eventually becomes

$$Q(t) = 1 - \hat{X}_e + 3\hat{X}_e^2 \int_0^1 \tau'^3(1-\tau')^2 d\tau' + 9\hat{X}_e^2 \int_0^1 d\tau' \times \int_0^{\tau'} d\tau''(1-\tau')^2 A(\tau',\tau'') + O\left(I_0^3\right), \quad (27)$$

where $A(\tau',\tau'')$ is given through Eq. (11). Notably, the last term in Eq. (27) has been estimated already in Eq. (13) and is equal to $\frac{9}{20}\hat{X}_e^2$. The coefficient of $\hat{X}_e^2$ eventually is computed as $\frac{3}{60} + \frac{9}{20} = \frac{1}{2}$, that is, the expected result.

It is worth noting that the present approach also can be applied to different convex shapes other than circles and spheres, provided the orientation of nuclei is the same (with a possible exception for triangles). This aspect has been discussed in detail in Refs. [25,26].

We conclude this section by quoting the recent results of Ref. [17]. In this noteworthy paper, the author faced the problem of describing the kinetics in terms of the actual nucleation rate. An ingenious application of the so called differential critical region approach makes it possible to find the $Q(t)$ kinetics by solving an appropriate integral equation [17]. On the other hand, the different method employed in the present paper, based on the use of the correlation function, pertains to the same class of stochastic approaches on which Kolmogorov's method is rooted. For the present topic, it could be enlightening to demonstrate that the two approaches are, in fact, equivalent.

IV. CONCLUSIONS

We have shown that, by employing the correlation function approach, the constraints on growth laws underlying the KJMA theory can be eliminated. In other words, the present modeling is not constrained to any form of growth law. The actual extended volume fraction is shown to be the natural variable of the kinetics, which implies universal curves. Besides, we proposed a formula to fit experimental data by using the measurable actual extended coverage. The displacement of the kinetics from the exponential law, i.e., the b parameter in Eq. (21), may give insight into the microscopic growth law of nuclei.

[1] A. N. Kolmogorov, Bull. Acad. Sci. USSR **3**, 355 (1937); *Selected Works of A. N. Kolmogorov*, edited by A. N. Shiryayev (Kluwer, Dordrecht, 1992), English translation, Vol. 2, p. 188.

[2] W. A. Johnson and R. F. Mehl, Trans. AIME **135**, 416 (1939).

[3] M. Avrami, J. Chem. Phys. **7**, 1103 (1939); **8**, 212 (1940); **9**, 177 (1941).

[4] M. J. Starink, Int. Mater. Rev. **49**, 191 (2004).

[5] J. Farjas and P. Roura, Phys. Rev. B **78**, 144101 (2008).

[6] R. A. Ramos, P. A. Rikvold, and M. A. Novotny, Phys. Rev. B **59**, 9053 (1999).

[7] P. Bruna, D. Crespo, R. Gonzalez-Cinca, and E. Pineda, J. Appl. Phys. **100**, 054907 (2006).

[8] A. V. Teran, A. Bill, and R. B. Bergmann, Phys. Rev. B **81**, 075319 (2010).

[9] A. Korobov, Phys. Rev. E **84**, 021602 (2011).

[10] A. Korobov, Phys. Rev. B **76**, 085430 (2007).

[11] M. Fanfoni and M. Tomellini, J. Phys.: Condens. Matter **17**, R571 (2005).

[12] S. Jun and J. Bechhoefer, Phys. Rev. E **71**, 011909 (2005); S. Jun, H. Zhang, and J. Bechhoefer, *ibid.* **71**, 011908 (2005).

[13] P. Karmwar, J. P. Boetker, K. A. Graeser, C. J. Strachan, J. Rantanen, T. Rades, Eur. J. Pharm. Sci. **44**, 341 (2011).

[14] J. Moller, Adv. Appl. Probab. **24**, 814 (1992); **27**, 367 (1995).

[15] T. Erhrdsson, J. Appl. Probab. **37**, 101 (2000).

[16] M. P. Shepilov, Glass Phys. and Chem. **30**, 291 (2004); Crystallogr. Rep. **50**, 559 (2005).

[17] N. V. Alekseechkin, J. Non-Cryst. Solids **357**, 3159 (2011).

[18] M. Tomellini and M. Fanfoni, Phys. Rev. B **55**, 14071 (1997).

[19] M. Fanfoni and M. Tomellini, Il Nuovo Cimento **20D**, 1171 (1998).

[20] N. G. Van Kampen, *Stochastic Processes in Physics and Chemistry* (North-Holland, Amsterdam, 1992).

[21] M. Tomellini, M. Fanfoni, and M. Volpe, Phys. Rev. B **65**, 140301 (2002).

[22] M. Fanfoni and M. Tomellini, Eur. Phys. J. B **34**, 331 (2003).

[23] T. Hill, *Statistical Mechanics* (Dover, New York, 1987).

[24] V. Sessa, M. Fanfoni, and M. Tomellini, Phys. Rev. B **54**, 836 (1996).

[25] M. Fanfoni, M. Tomellini, and M. Volpe, Phys. Rev. B **64**, 075409 (2001).

[26] A. Di Vito, M. Fanfoni, and M. Tomellini, Phys. Rev. E **82**, 061111 (2010).